CHAPTER IV

RESULTS AND DISCUSSION

4.1 Method evaluation

4.1.1 Calibration curves

Calibration curves for the leaf and the water were determined as following.

A 300 ml of each standard solution was spiked gradually into 2 g of leaf samples in a crucible. Also, 500 µl of internal standard was spiked. The leaf samples were then proceeded for leaf analysis as detailed in section 3.3.1 and 3.4. For water samples, the standard solution was spiked into a 2 L of deionized water and added 500 µl of internal standard, then extracted and concentrate to final volume 1 ml. PAH standard of leaf and water samples from above procedures was injected in three replicates onto the GC/FID column under the optimised conditions.

The calibration curve of each standard was constructed by plotting the area ratio between PAH peak area and internal standard peak area against spiked concentration of the PAH compounds. The results of calibration curves for leaf samples and water samples are shown in Appendix C. The linear regression equations obtained from the calibration curves are shown in Table 4-1 and Table 4-2. These calibration curves were used for calculating the amounts of the PAH compounds in the samples.

Table 4-1 Regression coefficients for the linear regression equations for the relationships between peak ratio and concentration in leaf samples

PAH	Slope	intercept	r^2
1. NAP	0.17	-47.27	0.78
2. ACY	0.23	-0.93	0.73
3. ACE	0.28	-7.27	0.91
4. FLU	0.33	-4.00	0.86
5. PHE	0.12	-1.40	0.85
6. ANT	0.50	-0.23	0.78
7. FLA	0.52	-0.62	0.92
8. PYR	0.25	-0.07	0.87
9. BaA	0.75	0.00	0.91
10. CHR	1.87	-0.01	0.91
11. BbF	0.35	-0.14	0.85
12. BkF	9.53	-0.08	0.82
13. BaP	4.14	-0.11	0.95
14. IP	0.22	-0.05	0.96
15. DbA	11.26	-0.01	0.96
16. BPER	389.91	-0.27	0.95

Table 4-2 Regression coefficients for the linear regression equations for the relationships between peak ratio and concentration in water samples

PAH	slope	intercept	r^2
1. NAP	0.64	-144.98	0.99
2. ACY	0.68	-16.22	0.99
3. ACE	0.69	-13.51	0.99
4. FLU	0.68	-6.54	0.99
5. PHE	0.66	-3.33	0.99
6. ANT	1.36	-0.22	0.94
7. FLA	0.69	-0.60	0.99
8. PYR	0.75	-0.88	0.96
9. BaA	0.09	-0.08	0.98
10. CHR	0.17	-0.03	0.96
11. BbF	0.14	-0.01	0.92
12. BkF	10.37	-0.32	0.88
13. BaP	0.16	-0.22	0.94
14. IP	0.48	+0.15	0.93
15. DbA	0.64	+0.001	0.71
16. BPER	1.92	+0.07	0.82

4.1.2 Retention time and Detection limit

An individual PAH in hexane was injected into GC/FID column under the optimal condition for five replicates to determine the retention time. The retention time and standard deviation are shown in Table 4-3.

The detection limit was constructed by plotting three times of standard deviation values against the area ratio for individual compound. Then the y-intercept value was used in the calibration curve to determine the concentration of detection

limit in leaf and water samples. The detection limits of leaf and water samples are shown in Table 4-4.

Table 4-3 The retention time of 16 PAH

PAH	Retention time (min)
1. NAP	5.04 (SD = 0.075)
2. ACY	7.70 (SD =0.086)
3. ACE	8.29 (SD =0.108)
4. FLU	10.13 (SD =0.080)
5. PHE	14.40 (SD =0.099)
6. ANT	14.50 (SD =0.055)
7. FLA	21.36 (SD =0.089)
8. PYR	23.09 (SD =0.161)
9. BaA	31.35 (SD =0.155)
10. CHR	31.63 (SD =0.014)
11. BbF	38.80 (SD =0.122)
12. BkF	38.97 (SD =0.054)
13. BaP	40.82 (SD =0.042)
14. IP	47.36 (SD =0.016)
15. DbA	47.71 (SD =0.124)
16. BPER	48.83 (SD =0.100)

Table 4-4 The detection limits of 16 PAH in leaf and water samples

PAH	Detection limits for leaf analysis (mg/kg)	Detection limits for water analysis (μg/L)
1. NAP	8.51	20.52
2. ACY	1.47	4.22
3. ACE	1.98	7.93
4. FLU	1.42	0.54
5. PHE	1.83	0.64
6. ANT	0.62	0.25
7. FLA	0.38	0.51
8. PYR	0.05	0.33
9. BaA	0.05	0.08
10. CHR	0.05	0.04
11. BbF	0.05	0.36
12. BkF	0.01	0.05
13. BaP	0.01	0.09
14. IP	0.01	0.05
15. DbA	0.01	0.005
16. BPER	0.01	0.009

The results from Table 4-4 shown that the detection limits in leaf samples ranged from 0.01 mg/kg for BPER to 8.51 mg/kg for NAP, and in water samples ranged from 0.005 μg/L for BkF to 20.52 μg/L for NAP. The results found that detection limit trend to decrease with increasing molucular weight of PAH.

4.1.3 Recoveries of PAH

The determination of recoveries of PAH compounds in leaf and water samples were carried out the same way as that from the calibration curves procedure (section 4.1.1). Recoveries of the compounds were calculated using the amounts of the compounds found as shown in Figure 4-1

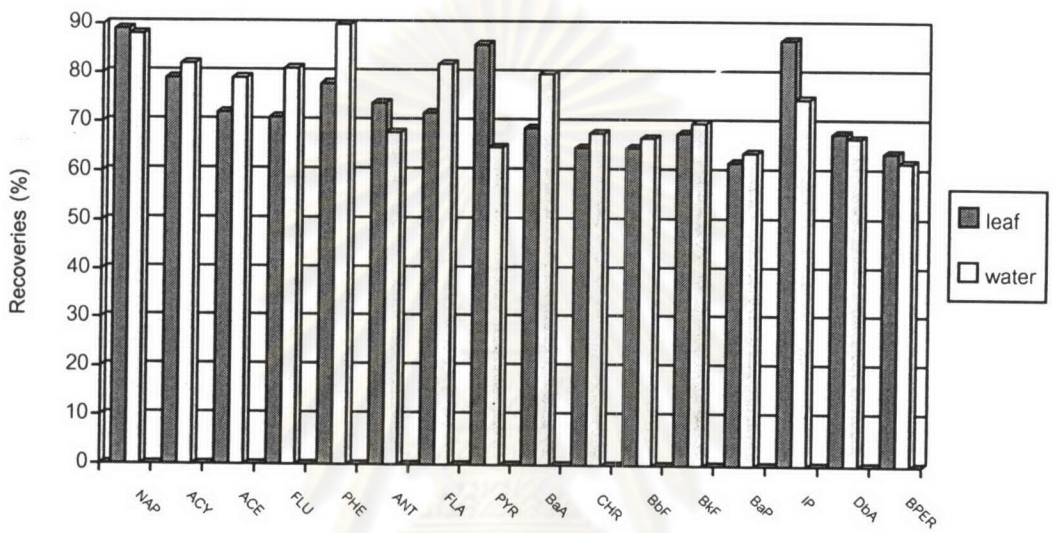

Figure 4-1 Average percent recoveries of 16 PAH in leaf and water samples

The results shown that %recoveries of leaf samples ranged from 62% in BaP to 89% in NAP. The remaining compounds including BaA, BPER, CHR, BbF, BkF and DbA were found to yield of 60 to 70% recovery, whereas ACY, ACE, FLU, PHE, ANT, FLA, PYR and IP were found to yield more than 70% recovery.

For water samples %recoveries are ranged from 62% in BPER to 90% in PHE. All of the remaining compounds had more than 60% recovery.

4.2 Partition coefficients of PAH in the leaf/water system

The experimental values of leaf/water partition coefficients (K_{LW}) and leaf lipid/water partition coefficients (K_{LLW}) were calculated, by using the results from leaf/water partitioning experiments. The key role of these experiment was on leaf lipid basis, so the K_{LW} was devided by leaf lipid fraction (0.067) which calculated from percentage of wax in section 3.7.2. The units of K_{LW} and K_{LLW} were L/kg, then they were converted to dimensionless by multiplying with ρ_L of 0.75 kg/L and ρ_{LLi} of 0.93 kg/L. The results of K_{LW} and K_{LLW} are shown in Table 4-5.

The density of leaf (ρ_L) was calculated from leaf mass (g) divided by volume of leaf (cm^3). Mass of leaves were weighed in four decimal places and volume of leaves were calculated using a planimeter and a vernia caliper to measure thickness and area of leaves. Leaf lipid density value (ρ_{LLi}) was assumed to be equivalent to the lipid density of hair (ρ_{HLi}).

Table 4-5 Average values of the dimensionless leaf/water partition coefficients (K_{LW}) and the leaf lipid/water partition coefficients (K_{LLW})

PAH	K_{LW} [a]	K_{LLW} [b]	log K_{LLW}
1. NAP	120	1,800	3.26
2. ACY	93	1,400	3.15
3. ACE	230	3,500	3.55
4. FLU	235	3,600	3.55
5. PHE	4,000	62,000	4.79
6. ANT	2,000	30,000	4.48
7. FLA	830	13,000	4.10
8. PYR	1,000	15,000	4.18
9. BaA	160	2,400	3.38
10. CHR	54	830	2.92
11. BbF	1,700	26,000	4.41
12. BkF	7,400	110,000	5.05
13. BaP	260	3,900	3.59
14. IP	5,700	85,000	4.93
15. DbA	26	400	2.60
16. BPER	74	1,100	3.05

Notes : [a] K_{LW} (dimensionless) = K_{LW} (L/kg) x ρ_L

[b] K_{LLW} (dimensionless) = (K_{LW} (L/kg) x ρ_{Li})/ leaf lipid fraction

ρ_L (g/cm^3) = mass(g) / volume(cm^3)

$$= \frac{\text{mass (g)}}{\text{area of leaf (cm}^2\text{) x thickness (cm)}}$$

$$= \frac{0.1072 \text{ g}}{7.22 \text{ cm}^2 \text{ x } 0.0198 \text{ cm}}$$

$$= 0.75 \text{ g/cm}^3 = 0.75 \text{ kg/L}$$

The experimental log K_{LLW} in this study were increased from NAP to ANT as shown in Table 4-5. These log K_{LLW} obtained were correlated with log K_{OW} and increased with the increasing of molecular weight of PAH. The high values of log K_{LLW} indicate that high bioaccumulation (WHO, 1998). However, PAH, with MW higher than 178 (ANT), the log K_{LLW} were not increased consistantly with log K_{OW}. This can be explained by the properties of PAH. That is extremely hydrophobic compounds tend to decrease in lipid solubility causing it difficult to measure and extract from leaves. Some of PAH may also lost during the partitioning experiments due to biodegradation, since leaves had a little sign of aging.

From the plots of log K_{LLW} with log K_{OW} of 16 PAH gave low correlation coefficient ($r^2 = 0.02$) as shown in Figure 4-2a. Howevere, excluding the values of compounds likely suspected of errors (BaA, CHR, BaP, DbA and BPER), a better correlation coefficients are obtained ($r^2 = 0.67$) as shown in Figure 4-2b.

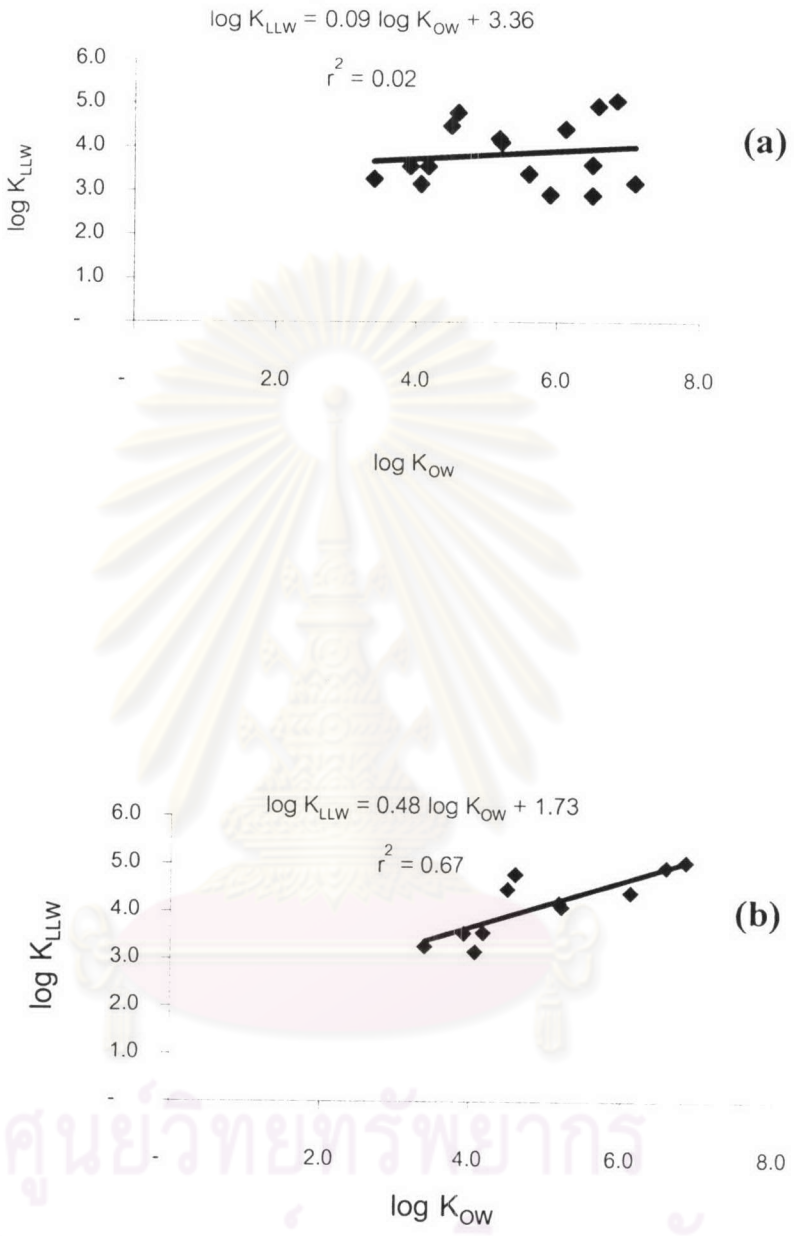

Figure 4-2 Plots of log K_{LLW} versus K_{OW} and their linear regression equations

The leaf lipid/water partition coefficients (K_{LLW}) can be compared with the fish/water partition coefficients (log K_{FW}), which has similar system with leaf lipid/water system (Table 4-6). Apparently most of log K_{FW} values are lower than that of log K_{LLW}. Due to higher metabolization of PAH in fish than in leaf lipid.

Table 4-6 Comparison of leaf lipid/water partition coefficients (K_{LLW}) with fish/water partition coefficients (K_{FW})

PAH	log K_{LLW} in this study	log K_{FW}*
1. NAP	3.26	2.50
2. ACY	3.15	-
3. ACE	3.55	2.59
4. FLU	3.55	3.26
5. PHE	4.79	-
6. ANT	4.48	3.01
7. FLA	4.10	2.58
8. PYR	4.18	-
9. BaA	3.38	2.54
10. CHR	2.92	3.74
11. BbF	4.41	-
12. BkF	5.05	4.12
13. BaP	3.59	3.42
14. IP	4.93	-
15. DbA	2.60	-
16. BPER	3.05	-

Source: * WHO, 1998

4.3 Partition coefficients of PAH in the leaf/air system (K_{LA})

The main uptake of hydrophobic compounds by plant leaves involves a partitioning process between the leaf and the surrounding media (Simonich and Hites, 1994) and lipid is the key role for this process. This is evident from several studies that the plant/air partition coefficient of a hydrophobic compound correlate with the quotient of lipid in the plants (Bakker et al., 2000).

Partition coefficients for the leaf/air system were calculated as follow:

$$K_{LA} = C_L/C_A \quad (4.1)$$

From Equation 1.6 and 1.7, substituting C_L/C_W with K_{LW} and converting H to dimensionless a factor of RT = 2.35 $kPam^3/mol$ (Muller et al., 1994) was used, then

$$K_{LA} = 2.35K_{LW}/H \quad (4.2)$$

$$K_{LLA} = 2.35K_{LLW}/H \quad (4.3)$$

The results are shown in Table 4-7

Table 4-7 Average values of the dimensionless leaf lipid/air partition coefficients (K_{LLA}) in this study

PAH	K_{LLA}	log K_{LLA}
1. NAP	$96x10^3$	4.98
2. ACY	$40x10^4$	5.60
3. ACE	$65x10^4$	5.82
4. FLU	$110x10^4$	6.03
5. PHE	$190x10^5$	7.29
6. ANT	$96 x10^5$	6.98
7. FLA	$35 x10^5$	6.54
8. PYR	$42 x10^5$	6.62
9. BaA	$60 x10^4$	5.77
10. CHR	$20 x10^4$	5.27
11. BbF	$60 x10^5$	6.77
12. BkF	$390 x10^{12}$	13.59
13. BaP	$640 x10^9$	11.80
14. IP	-	-
15. DbA	$290 x10^9$	11.46
16. BPER	$230 x10^9$	11.36

The experimental log K_{LLA} in this study were increased from NAP to PHE (as shown in Table 4-7) and correlated with log K_{OA} from the literature. But log K_{LLA} of PAH from ANT to BkF were not correlated with log K_{OA} values. This is similar to the case of log K_{LLW} which were not increased consistantly with log K_{OW}. While octanol/air system is similar to lipid/air system, the relationship between log K_{OA} and log K_{LLA} would be expected (Figure 4-3a). The linear regression equations of the relationships between log K_{LLA} and log K_{OA} from this experiment gave, the slope and the intercept of 0.99 and –0.84 respectively and r^2 of 0.51. But if the values of those

log K_{LLA} (ANT, FLA, PYR, BaA, CHR and BbF) were neglected, the correlation coefficient would increase to 0.86 as shown in Figure 4-3b.

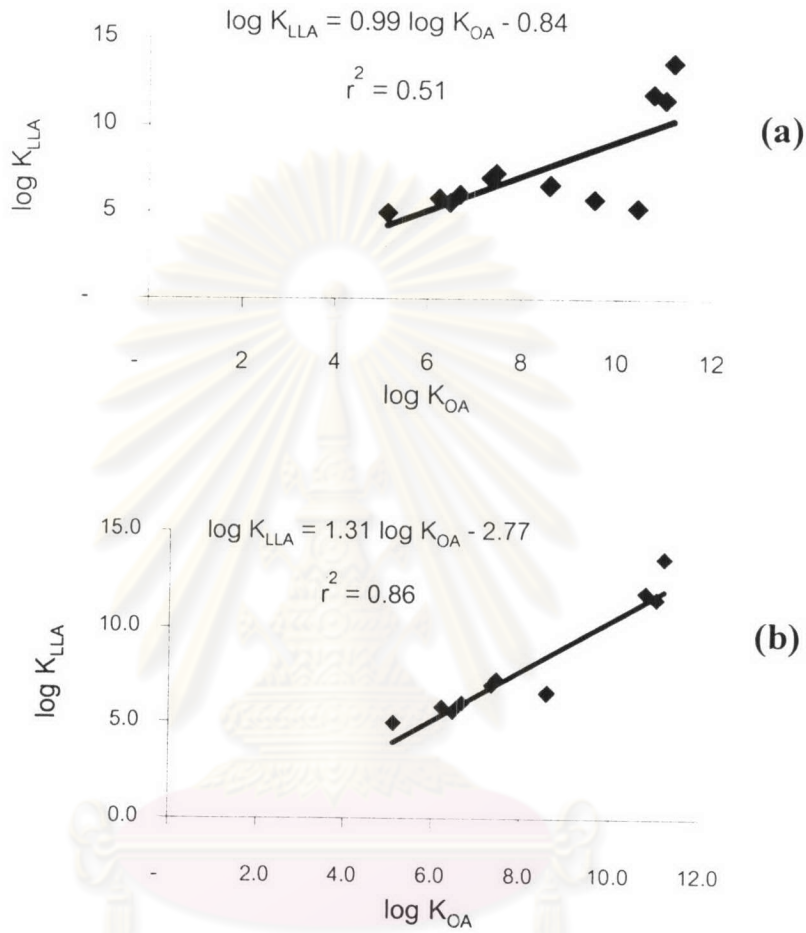

Figure 4-3 Plots of log K_{LLA} versus log K_{OA} and the linear regression equations

The slope obtained (0.99) is considered to be close to one. In many experiments the high correlation between air-to-plant concentration factors (K_{PA}) and the K_{OA} is demonstrated, which means that the air-to-plant lipid and air-to-octanol systems are similar. According to the theory, if the slope of a plot of log K_{PA} versus K_{OA} is equal to one, K_{PA} and K_{OA} are linearly related and the lipid fraction of the plant behaves as octanol (Bakker et al., 2000).

Considering of the slope between log K_{LLA} and log K_{OA} from this study and from the literature (as shown tn Table 4-8), plots of log K_{PA} versus log K_{OA} for a number of plant species give various slopes. For example, in a field experiment, a slope of the log-log plot for PAH in needle, leaves and tree bark of 0.48 was observed (Simonich and Hites, 1994). Thomas et al., (1998) studied the concentration of PCB in a field pasture and found that the slope amounted to 0.4. While Komp and McLachlan (1997) and Bohme et al. (1999), studied uptake of SOC in different plant species and found different slopes over species (shown in Table 4-8). According to them the differences of such slopes were attributed to the differences in lipid quality (Komp and McLachan, 1997). Another explanation for shallow slopes of the log-log plots is a deviation from equilibrium, leading to greater underestimations of K_{PA}'s of the compounds with higher K_{OA} values.

Table 4-8 Slopes and correlation coefficients of plots of log K_{PA} ($C_{vegetation}/C_{gaseous\ phase}$) versus log K_{OA} from several studies

Plant	Compounds	Experiment	Slope	r^2	reference
Ryegrass	PCB, CB and PAH	lab	1.00	0.95	Toll and McLachlan,1994
Azalea	PTC, PCB and CB	lab	0.91	0.85	Paterson et al., 1991
needles, leaves, seed, tree bark	PAH	field	0.48	0.98	Simonich and Hites, 1994
Pasture	PCB	field	0.32-0.47	0.66-0.96	Thomas et al., 1998
Ryegrass	PCB	lab	1.15	0.98	Komp and McLachlan, 1997
Plantain	PCB	lab	0.87	0.98	Komp and McLachlan, 1997
Yarrow	PCB	lab	0.57	0.93	Komp and McLachlan, 1997
Clover	PCB	lab	0.70	0.86	Komp and McLachlan, 1997
Ryegrass	PCB, CB and PAH	field	0.60	0.93	Bohme et al., 1999
Plantain	PCB, CB and PAH	field	0.65	0.96	Bohme et al., 1999
Sunflower	PCB, CB and PAH	field	0.39	0.85	Bohme et al., 1999
Corn	PCB, CB and PAH	field	0.57	0.90	Bohme et al., 1999
White clover	PCB, CB and PAH	field	0.66	0.90	Bohme et al., 1999
lady's mantle	PCB, CB and PAH	field	0.53	0.95	Bohme et al., 1999
Dandelion	PCB, CB and PAH	field	0.78	0.98	Bohme et al., 1999

4.4 Concentrations of PAH in leaf samples (C_L)

The results of the concentrations of PAH compounds detected in leaf samples are shown in Table 4-9

Table 4-9 Concentrations of the PAH in leaf samples (C_L) from four study sites

PAH	PAH in leaf samples (mg/kg)			
	Patumwan	Saphan Khwai	Phongphet	Kasemraj
1. NAP	ND	ND	ND	ND
2. ACY	4.84	5.13	4.52	6.39
3. ACE	26.12	26.81	26.25	26.55
4. FLU	13.25	19.67	12.83	13.03
5. PHE	13.64	14.33	14.25	15.12
6. ANT	0.91	3.75	1.95	1.52
7. FLA	1.68	3.22	1.81	1.99
8. PYR	2.36	5.73	2.54	3.23
9. BaA	0.14	1.92	0.25	1.45
10. CHR	0.22	0.54	0.19	0.67
11. BbF	0.45	0.55	0.48	0.50
12. BkF	ND	0.01	ND	0.01
13. BaP	0.14	ND	0.20	ND
14. IP	0.24	0.23	ND	ND
15. DbA	ND	0.56	0.32	0.24
16. BPER	ND	0.01	ND	0.01
Total PAH	**63.99**	**82.46**	**65.59**	**70.71**

Note : ND = Non detectable

From Table 4-9 ACE is dominant in leaves from all four sites (26.12 - 26.81 mg/kg), followed by FLU and PHE (12.83 - 19.67 and 13.64 - 15.12 mg/kg), respectively. While the concentration of PAH in leaf samples with higher molecular weight than BaA (MW=228.3) were lower than 1 mg/kg (0.14-0.45, 0.01-0.56, 0.19-0.48 and 0.01-0.67 mg/kg from Patumwan, Saphan Khwai, Phongphet and Kasemraj, respectively). The data indicates that most of the PAH, which found in orange jasmine leaves was taken up by absorption from the vapor phase (Nakajima et. al., 1995). Total concentrations of PAH in leaf samples, which collected from four study sites were shown in Figure 4-4, and found that total PAH at Saphan Khwai was the highest (82.46 mg/kg), while Kasemraj and Phongphet were slightly difference (70.71 and 65.59 mg/kg, respectively). While Patumwan area was considerably the lowest (63.99 mg/kg). This indicates that the PAH concentrations in leaf samples may vary according to the influence of traffic density (traffic volume) since vehicle exhaust seems to be the major source of PAH. Saphan Khwai site has highest concentrations of total PAH because Saphan Khwai is the residential area and surrounded by commercial buildings, which usually has high traffic volume and traffic jam. However, plot of total PAH against traffic volume (Figure 4-5) indicate no relationship. This is probably due to other factors, i.e. vehicle condition, traffic stoppage, type of fuel, wind direction.

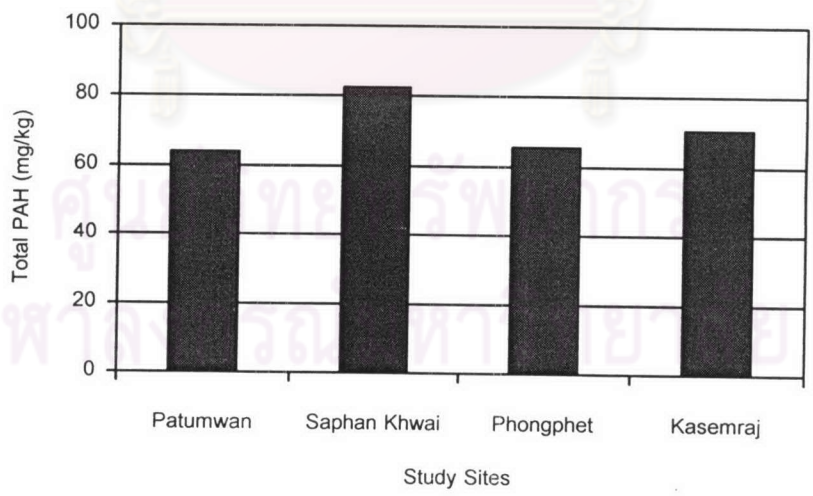

Figure 4-4 Total PAH in leaves collected from four sites in Bangkok

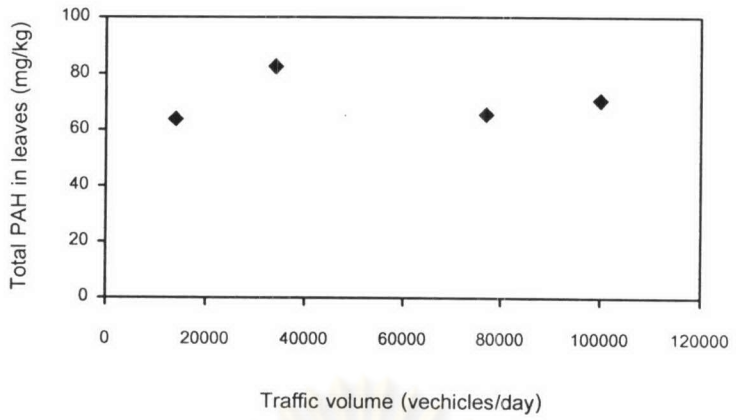

Figure 4-5 Plots of total PAH in leaves versus traffic volume

From the concentrations of PAH in leaf samples (Table 4-8), the concentration of PAH in air can be calculated (described as calculated air concentration, C_{Acal}) using Equation 4.5 and the K_{LLA} in Table 4-7:

$$C_{A\,cal} = C_L\ (mg/kg) / K_{LLA}\ (dimensionless) \qquad (4.4)$$

A units of C_{Acal} from above were changed into ng/m^3,by mutiplying with air density of $1.19x10^6$ mg/m^3 (at 25°C) (Simonich and Hites, 1994).

4.5 Comparison of the calculated and measured atmospheric PAH

The potential of leaves as bioindicator of atmospheric PAH, could be studied by comparing the calculated PAH concentration estimated from the orange jasmine leaves and the concentrations of atmospheric PAH which collected from the same locations by high volume air sampler. The atmospheric PAH from the air (described as measured air concentration, C_{Amea}) in this study were obtained from Benjalak Karnchanasest, 2003. The comparison of calculated and measured air concentrations (C_{Acal} and C_{Ames}) are shown in Table 4-10

Table 4-10 Calculated (C_{Acal}, ng/m^3) and measured (C_{Amea}, ng/m^3) atmospheric PAH

PAH	Patumwan		Saphan Khwai		Phongphet		Kasemraj	
	C_{Acal}	C_{Amea}	C_{Acal}	C_{Amea}	C_{Acal}	C_{Amea}	C_{Acal}	C_{Amea}
1. NAP	ND	ND	ND	ND	ND	ND	ND	ND
2. ACY	14.44	13.05	15.29	16.8	13.47	15.57	19.06	19.86
3. ACE	47.41	13.05	48.67	19.97	47.65	15.52	48.2	16.76
4. FLU	14.81	6.42	21.98	10.7	14.33	7.63	14.56	8.37
5. PHE	0.84	5.15	0.88	11.55	0.87	7.41	0.93	12.36
6. ANT	0.11	0.41	0.46	2.56	0.24	1.95	0.19	0.93
7. FLA	0.58	1.31	1.11	1.88	0.63	0.55	0.69	1.16
8. PYR	0.67	0.56	1.64	1.60	0.72	0.47	0.92	1.66
9. BaA	0.28	0.08	3.85	1.13	0.5	0.22	2.91	2.67
10. CHR	1.43	0.06	3.46	0.18	1.23	0.10	4.3	0.13
11. BbF	0.15	0.30	0.34	1.55	0.22	0.29	0.29	2.82
12. BkF	ND	0.03	3.70×10^{-10}	0.12	ND	ND	4.52×10^{-10}	0.69
13. BaP	2.66×10^{-7}	0.26	ND	0.64	3.75×10^{-7}	0.04	ND	0.06
14. IP	ND	3.70	ND	0.45	ND	0.25	ND	0.26
15. DbA	ND	ND	1.14×10^{-6}	0.62	6.68×10^{-7}	0.49	4.94×10^{-7}	0.44
16. BPER	ND	0.008	2.60×10^{-8}	0.001	ND	0.003	8.86×10^{-9}	ND

From Table 4-10, there are only 10 PAH both in the leaves and in the air that can be plotted. The measured concentrations of PAH in the air plotted against their calculated concentrations are shown in Figure 4-6, and the linear regression equations are shown in Table 4-11.

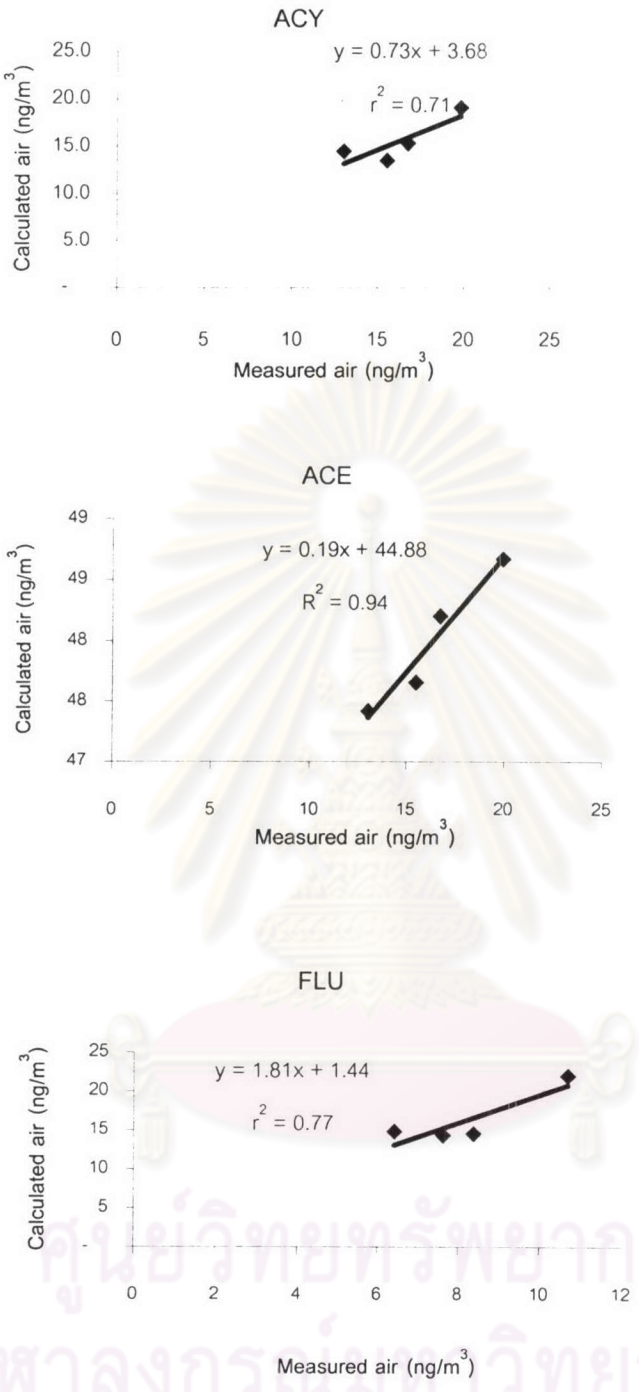

Figure 4-6 Plots of C_{Acal} versus C_{Amea} and the linear regression equations

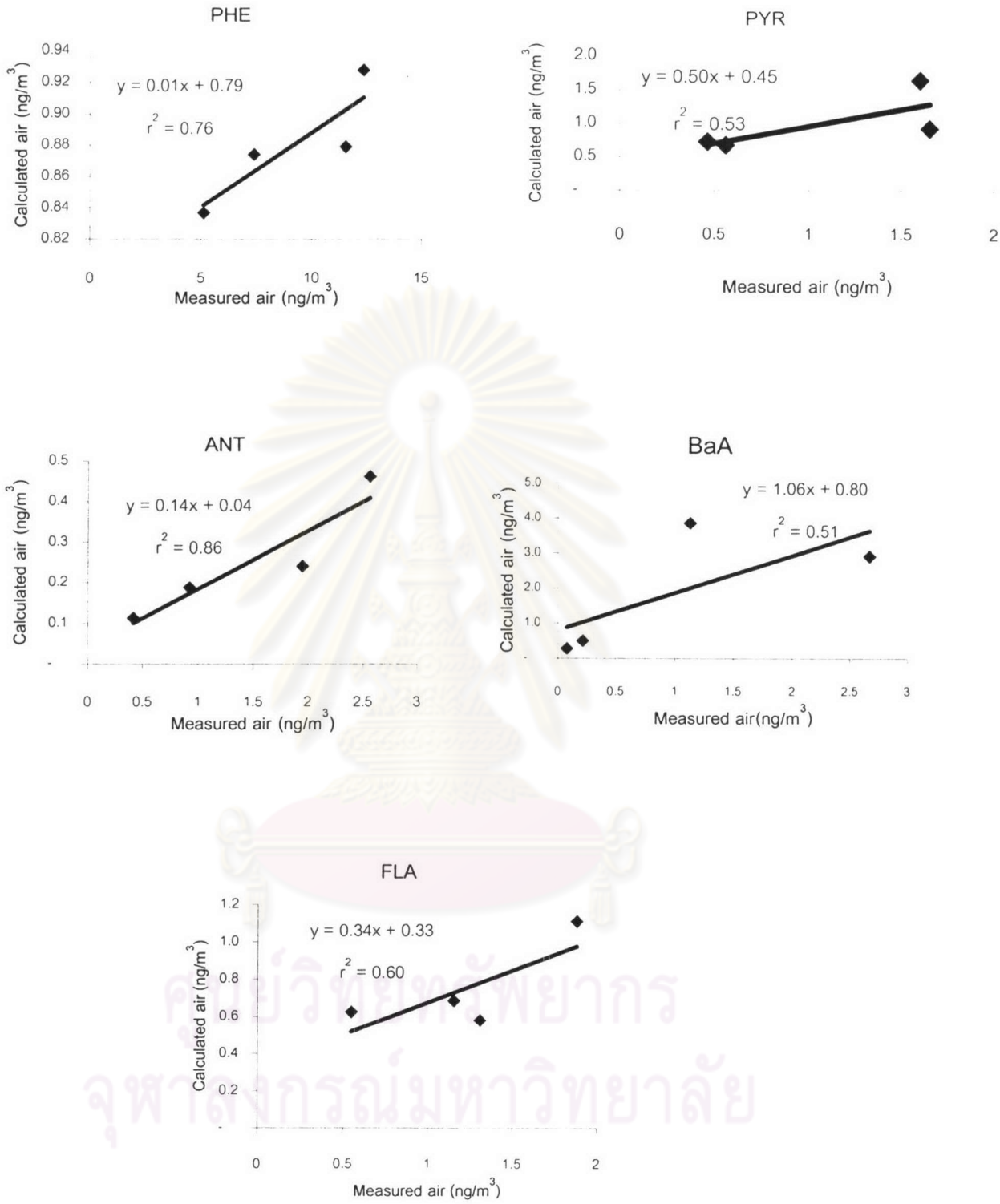

Figure 4-6 Plots of C_{Acal} versus C_{Amea} and the linear regression equations (continued)

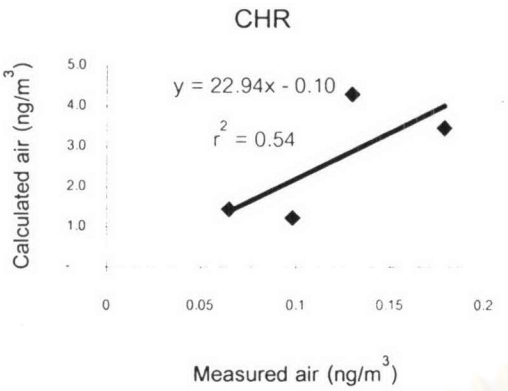

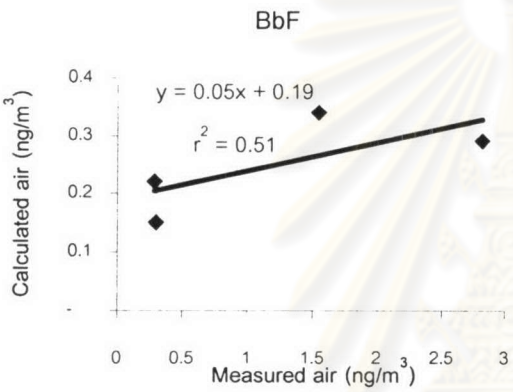

Figure 4-6 Plots of C_{Acal} versus C_{Amea} and the linear regression equations (continued)

Table 4-11 Slope and correlation coefficients of plot of C_{Acal} versus C_{Ames}

PAH	Slope	intercept	r^2
2. ACY	0.73	3.68	0.71
3. ACE	0.19	44.88	0.94
4. FLU	1.81	1.44	0.77
5. PHE	0.01	0.79	0.76
6. ANT	0.14	0.04	0.86
7. FLA	0.34	0.33	0.60
8. PYR	0.50	0.45	0.53
9. BaA	1.06	0.80	0.51
10. CHR	22.94	-0.10	0.54
11. BbF	0.05	0.19	0.51

From Table 4-11 the regression analysis of relationships between calculated and measured PAH in the air was clearly shown good linear relationships ($r^2 > 0.70$, p-value = 0.028) for lower MW, since lower MW PAH were relatively high vapor pressure and mostly presented in gas phase. While the concentration of higher MW PAH which mostly occurred in particulate phase have low correlation coefficient ($r^2 \sim 0.5$, p-value = 0.230). This difference seems to reflect the difference in vapor pressure based on molecular weight. Plant leaves are presumed to take up PAH in the atmosphere by either attachment of suspended particulate matter (SPM) onto leaves with permeation of PAH into the cuticles from the attached SPM or adsorption onto leaves of vapor phase PAH. The uptake of PAH via roots into the leaf is negligible, because lipophilic xenobiotics cannot migrate such a long distance in plant tissue, as reported by many investigators (Nakajima et al., 1995; Kylin et al., 1994). Particle phase PAH may be subjected to washoff and windblow, whereas this may not apply for gas phase PAH taken up by adsorption/absorption by the plant cuticle (Smith, Thomas and Jones, 2001).